THE JOURNAL OF PHYSICAL CHEMISTRY Letters

pubs.acs.org/JPCL Letter

M11plus, a Range-Separated Hybrid Meta Functional Incorporating Nonlocal Rung-3.5 Correlation, Exhibits Broad Accuracy on Diverse Databases

Benjamin G. Janesko,* Pragya Verma, Giovanni Scalmani, Michael J. Frisch, and Donald G. Truhlar

Cite This: J. Phys. Chem. Lett. 2020, 11, 3045−3050 Read Online

ACCESS | Metrics & More | Article Recommendations | Supporting Information

ABSTRACT: We present tests of the recent M11plus Minnesota density functional for a broad range of main-group and transition-metal chemistry databases, most of which were not used in in the construction of any of the Minnesota functionals. M11plus is a range-separated hybrid meta functional combining long-range nonlocal Hartree−Fock exchange with nonlocal rung-3.5 correlation. M11plus performs well for main-group thermochemistry, kinetics, and noncovalent interactions and especially well for radical species. It is numerically well behaved, it has a computational cost that is ∼1.2 to 1.5 times that of M11 in realistic calculations, and it is particularly accurate for triplet excited states, which is a difficult challenge for density functional approximations. The results show that nonlocal rung-3.5 correlation is a broadly useful ingredient for improving the performance of density functional approximations.

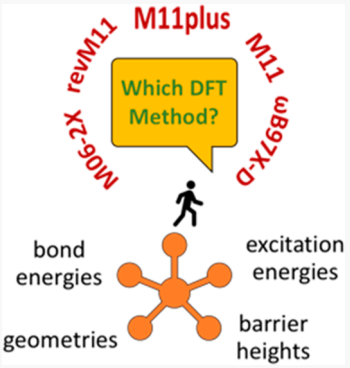

Kohn−Sham density functional theory (DFT)[1] would be exact if it incorporated the exact exchange-correlation (XC) functional. However, the exact functional is unobtainable, and practical DFT calculations use approximate XC functionals. The clear path to improving the accuracy of these calculations is to improve the approximation to the XC functional. This can be done by improving the functional form, adding new ingredients, enforcing relevant known constraints, and parametrizing to broad databases. The earliest proposed approximate functionals depended on two local ingredients: spin densities[1,2] and the magnitudes of their gradients.[3] (We classify ingredients as local if the energy density at a point in space depends only on quantities evaluated at that point, or their derivatives with position, exemplified by spin-density gradients and local spin-orbital-dependent kinetic energy density. Nonlocal ingredients require information over a finite or infinite region to calculate the energy density at a point.) Adding all[4] or some portion[5] of nonlocal spin-orbital-dependent Hartree−Fock exchange and local kinetic energy densities[6,7] was a key step in improving the performance of approximate XC functionals. However, balancing local approximations to correlation with nonlocal exchange has been an ongoing challenge.

Local models for correlation usually are functions of only spin densities, the magnitudes of their gradients, and the spin−orbital-dependent kinetic energy density, all of which depend only on occupied orbitals. Some progress has been made with correlation functionals involving densities at two points[8] or involving both occupied and unoccupied orbitals (e.g., doubly hybrid functionals).[9,10] Nonlocal correlation functionals of only the occupied orbitals have been less widely explored. Notable examples include Becke's method of modeling static correlation in terms of the exchange hole[11] and the rung-3.5 strategy[12−14] of modeling correlation using the expectation values of nonlocal one-electron operators.

Our recent functional, M11plus,[15] has a new combination of ingredients: spin densities, the magnitudes of their gradients, spin-specific kinetic energy densities, 100% long-range nonlocal Hartree−Fock exchange, a fraction of short-range nonlocal Hartree−Fock exchange, and two kinds of rung-3.5 nonlocal correlation—one inspired by local hybrid functionals[16] and one inspired by Becke's static correlation model,[17] both constructed from nonlocal one-electron ingredients. (The "plus" in M11plus denotes the addition of the rung-3.5 correlation). The original M11plus paper[15] was encouraging, showing good accuracy, competitive computational cost, and good self-consistent field (SCF) convergence. Here we validate M11plus more broadly, first by tests against databases and then by the examination of second-order response properties and computational timings. First, we present a test of several functionals against two ground-state databases and two excited-state databases. The functionals

Received: February 19, 2020
Accepted: March 25, 2020
Published: March 25, 2020

https://dx.doi.org/10.1021/acs.jpclett.0c00549
J. Phys. Chem. Lett. 2020, 11, 3045−3050

tested include functionals previously found best for a large database (vide infra) plus M11plus and three other Minnesota functionals, namely M06-2X,[18] M11,[19] and revM11.[20] Second, we examine response properties (polarizabilities and local force constants) in stretched covalent bonds to confirm "well-behaved" treatment. Finally we report computational timings for realistic force and frequency calculations on polyalanine oligomers Ala_9 and Ala_{25}.

Ground-State Databases. To benchmark the performance for ground states, we consider the general main-group thermochemistry, kinetics, and noncovalent interaction database GMTKN55[21] consisting of 55 separate data sets as well as the metal−organic reactions database MOR41[22,23] consisting of 41 reaction energies of closed-shell organometallic complexes. We compare this to the six occupied-orbital-only functionals giving the lowest weighted total mean absolute deviation (WTMAD-2) previously reported for the entire GMTKN55 set: the Minnesota functionals, M05-2X-D3(0),[24−26] M06-2X, and M08-HX;[27] the range-separated hybrid gradient functional, ωB97X-D3(0);[28] and the range-separated hybrid gradient and meta functionals, ωB97X-V[29] and ωB97M-V,[30] respectively, both of which incorporate two-point-density corrections. Note that the functionals with the suffix D3(0) incorporate molecular-mechanics-damped dispersion terms that go to zero at short-range. All calculations use basis sets, geometries, and reference values taken from the literature (Section SI-1), enabling a direct comparison to published benchmarks.

Table 1 summarizes the weighted total mean absolute deviation (WTMAD-2) on GMTKN55 and the root-mean-square deviation (RMSD) on MOR41, as compared to the "best" functionals (whose selection is previously explained) from published benchmarks. The top part of the table gives literature results,[21−23,31] and the bottom part gives our calculations. Section SI-4 reports error statistics from the 55 separate data sets in GMTKN55. Section SI-5 reports M11 and M11plus total energies and energy differences from all species in GMTKN55. The M11plus WTMAD-2 value of 4.99 kcal/mol places it squarely in the ranks of the "best" functionals. We find that M11plus offers a performance that is comparable to the most accurate previous Minnesota functionals while also including 100% long-range exact nonlocal exchange that improves excitation energies (*vide infra*). Section SI-4 shows that M11plus gives a mean absolute error (MAE) lower than the parent M11 and revM11 functionals, which do not include nonlocal rung-3.5 ingredients, for 33 and 34 of the 55 data sets, respectively. By way of comparison, the long-range-corrected two-point-density nonlocal correlation functional ωB97M-V gives an MAE that is lower than the parent ωB97X-V functional, which does not include meta ingredients, for 32 of the 55 data sets. This comparison shows that adding a nonlocal rung-3.5 correlation to a state-of-the-art long-range-corrected meta functional M11 has an impact that is at least comparable to adding meta ingredients to a state-of-the-art long-range-corrected functional ωB97X-V. Results for MOR41 are consistent with this; M11plus provides an RMSD that is comparable to or below any of the other tested functionals, except for those (in the first two rows) that contain a two-point-density nonlocal correlation.

The authors of the GMTKN55 database partitioned it into five subsets: basic properties and reaction energies of small systems, reaction energies for large systems and isomerization reactions, reaction barrier heights, intermolecular noncovalent interactions, and intramolecular noncovalent interactions. Table 2 reports the performance for these five subsets. M11plus and revM11 improve upon M11 for both the noncovalent subsets, indicating better capture of the medium-range correlation energy. M11plus performs particularly well for the reaction energies of large systems, driven in part by its previously reported[15] good performance for the RSE43 database of radical stabilization energies, which comprises 43 of the 243 data in this subset. This good performance comes despite M11plus not being accurate for the MB16-43 "mindless benchmark" database, which comprises another 43 of the 243 data in the large system subset. The M11plus RMSD of 38.0 kcal/mol for the mindless set is, however, close to the ωB97X-V and ωB97X-D3(0) RMSDs of 38.1 and 41.8 kcal/mol for this set. M11plus also performs very well for the SIE4x4 database, which comprises 16 of the 473 data in the basic properties subset and which involves one-electron self-interaction error; here M11plus outperforms most of the other "best" functionals. (See Section SI-4.)

The nonlocal rung-3.5 correlation in M11plus is designed to mitigate the trade-off in most previous functionals between the performance for closed shells and that for open-shell radicals. The success of M11plus in this regard was shown in our previous work, where it improved on its predecessors for the MR53 multireference database, the SIE4x4 self-interaction error database, and the RSE43 radical stabilization energy database. However, the GMTKN55 database has only a small amount of multireference character, with only 13 of its 55 data sets including any open-shell systems, and consequently, the

Table 1. Error Statistics (kcal/mol) for Benchmark Databases of the General Main-Group Thermochemistry, Kinetics, and Noncovalent Interactions Database GMTKN55 and the Closed-Shell Metal-Organic Reactions Database MOR41[a]

method	GMTKN55, WTMAD-2	MOR41, RMSD
ωB97M-V	3.53[b]	2.6[c]
ωB97X-V	3.98[d]	2.8[e]
M05-2X-D3(0)	4.61[d]	N/A
ωB97X-D3(0)	4.77[d]	5.2[e,f]
M06-2X	4.89[d]	8.8[e]
M08-HX	5.30[d]	N/A
M11	6.92[d]	5.3[e,g]
M06-2X	4.76	8.7
M11	6.90[h]	5.9
revM11	5.72	5.2
M11plus	4.98	4.6

[a]Results above the blank row are taken from the literature; results below the blank row are new calculations. All the GMTKN55 calculations in this table use the def2-QZVP basis set with additional diffuse functions for the G21EA, WATER27, AHB21, and IL16 sets. Except where noted otherwise in footnote *f* all the MOR41 calculations in this table use the def2-QZVPP basis. [b]Ref 31. [c]Ref 23. [d]Ref 21. [e]Ref 22. [f]D3(BJ) dispersion. [g]This literature value was obtained with the smaller def2-TZVPP basis set; we obtain an error of 5.2 kcal/mol when we redo our own calculations with the smaller basis set. [h]Our calculations use spin-symmetry-broken singlet states for five of the molecules in the W4-11 set (B_2, BN, C_2, CF, OF), one molecule in the RC21 set (2p2), and one molecule in the G2RC set (singlet CH_2), contributing to a WTMAD-2 value for M11 on the GMTKN55 database that is slightly lower than the one reported previously.

https://dx.doi.org/10.1021/acs.jpclett.0c00549
J. Phys. Chem. Lett. 2020, 11, 3045−3050

Table 2. WTMAD-2 (kcal/mol) for Subdatabases of the GMTKN55 Database[a]

	partition 1					partition 2	
method	basic properties of small systems	reaction energies of large systems	barrier heights	intermolecular noncovalent interactions	intramolecular noncovalent interactions	Radical7[b]	Nonradical48[c]
ωB97M-V[d]	2.73	4.79	3.40	2.90	4.53	5.99	3.18
ωB97X-V[e]	3.34	6.68	4.21	3.03	3.62	5.45	3.76
M05-2X-D3(0)[e]	2.73	5.84	4.99	5.20	7.48	4.62	4.63
ωB97X-D3(0)[e]	3.32	7.85	4.67	4.54	4.86	6.28	4.56
M06-2X[e]	2.73	6.14	4.98	5.51	6.64	4.33	4.94
M08-HX[e]	2.75	5.67	3.32	7.11	8.55	3.84	5.44
M11[d]	3.15	7.27	4.44	10.08	11.12	5.70	7.07
M06-2X	2.71	6.22	3.72	5.59	6.70	4.46	4.80
M11	3.13	7.28	4.47	9.97	11.15	5.74	7.05
revM11	3.58	8.13	5.82	4.90	7.99	4.98	5.81
M11plus	3.77	4.91	4.43	5.43	6.87	3.13	5.20

[a]Results in the first seven rows are taken from the literature; results in the last four rows are new calculations. [b]G21EA, G21IP, SIE4x4, ALKBDE10, HEAVYSB11, RC21, and RSE43 data sets. [c]All GMTKN55 data sets not in Radical7. [d]Ref 31. [e]Ref 21.

error statistics for the full database do not clearly display this strength of M11plus. To address this, the last two columns of Table 2 show a new partition of the GMTKN55 database; in particular, we divide it into the Radical7 and Nonradical48 subdatabases. The former comprises seven data sets emphasizing radical species (G21EA for electron affinities, G21IP for ionization potentials, SIE4x4 for self-interaction error, ALKBDE10 for alkyl homolytic bond dissociations, HEAVYSB11 for heavy-atom hydride homolytic bond dissociations, RC21 for radical cation chemistry, and RSE43 for radical stabilization energies), and the latter comprises the remaining 48 data sets. Table 2 shows that M11plus combines the excellent accuracy of Radical7 with the good performance of Nonradical48.

Figure 1 shows the weighted total mean absolute deviation for Radical7 versus those for Nonradical48 for M11plus and all

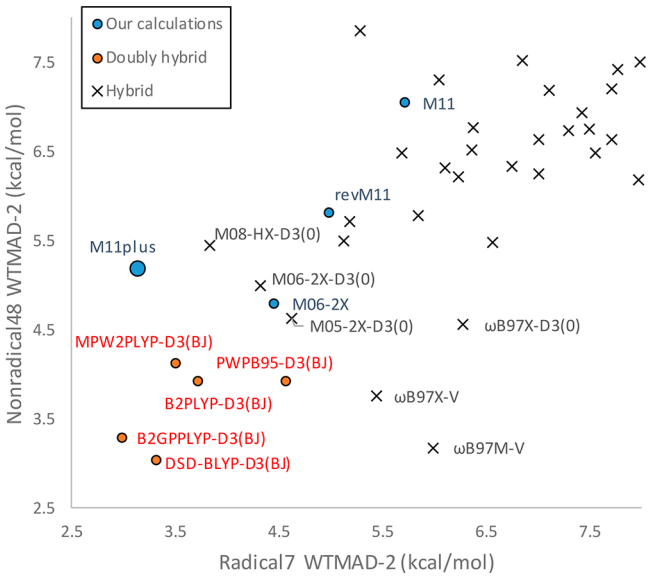

Figure 1. Weighted total mean absolute deviation (WTMAD-2 in kcal/mol) for Radical7 versus those for Nonradical48. "Our calculations" are functionals treated in this work; other functionals are evaluated from the MADs of individual databases reported in refs 21 and 31. Selected functionals are labeled; data for all functionals are available in the Supporting Information.

of the dispersion-corrected hybrid and doubly hybrid functionals reported in refs 21 and 31. Only M11plus (which involves only occupied orbitals) and the doubly hybrid functionals (which involve unoccupied orbitals) overcome the radical/nonradical trade-off so that they appear in the lower left corner of the figure. The errors for all occupied-orbital-only functionals other than M11plus show a clear trade-off in performance for the two data sets, with low WTMAD-2 for Radical7 (e.g., M08-HX-D3(0)) coming at the expense of higher WTMAD-2 for Nonradical48. We conclude that a special strength of M11plus is that it provides combined accuracy for both radicals and closed-shell species.

Excited-State Databases. For excited states, we consider two databases. The first electronic excitation database is a set of 103 singlet and 63 triplet valence excitations of 28 organic molecules (hydrocarbons, aromatics, carbonyls, and nucleobases) for which Schreiber et al. calculated CC3 and CASPT2 reference data.[32] Whereas the CC3 method is very accurate (~0.03 eV), the use of CASPT2 for some reference data may cause larger errors.[33] The second electronic excitation database is the lowest singlet and triplet excitations of 11 captodative chromophores, for which Grotjahn et al.[34] calculated CC2 reference data. (CC3 and CC2 are perturbative approximations to EOM-CCSDT and EOM-CCSD, respectively.) The CC2 method is expected to have an accuracy of ~0.2 eV for the captodative database because the ground states do not have significant multireference character and the excitations do not have significant double-excitation character.[33−35]

For excited states, we compare three functionals, M06-2X, ωB97X-D,[36] and Lh-SsifPW92,[37] which are, respectively, the global hybrid, the range-separated hybrid, and the local hybrid, giving in ref 38 the lowest MAE for triplet excitations in the set by Schreiber et al. (Note that Lh-SsifPW92 is called Lh12ct-SsifPW92 in ref 34.) The Lh-SsifPW92 and M06-2X functionals also gave the lowest MAE for excitation of the lowest-energy triplets of the captodative species.[34] All calculations use basis sets, geometries, and reference values taken from the literature (Section SI-1), enabling a direct comparison to published[34,38] benchmarks. Section SI-6 reports reference, M11, and M11plus state symmetries and energies for all excitations in the set by Schreiber et al. Section SI-7 reports excitations of the singlet fission chromophores.

https://dx.doi.org/10.1021/acs.jpclett.0c00549
J. Phys. Chem. Lett. 2020, 11, 3045−3050

Table 3 summarizes the error statistics for the singlet and triplet valence excited states considered here. M11plus outperforms M11 and revM11 for the Schreiber et al. set of triplet excited states, and it gives an MAE that is competitive with the best published results. The triplet performance is even more outstanding for the captodative chromophores, where the MAE of M11plus for the triplets is lower than that of any functional in the previous[34] study.

Table 3. Mean Absolute Errors (eV) for Singlet and Triplet Valence Excitations[a]

method	medium-sized organic molecules: 103 singlets, 63 triplets	singlet fission chromophores: 11 first singlets, 11 first triplets
Lh-SsifPW92	0.33, 0.16[b]	0.18, 0.50[c]
M06-2X	0.33, 0.23[b]	0.08, 0.47[c]
ωB97X-D	0.29, 0.32[b]	0.10, 0.71[c]
M06-2X	0.38, 0.25	0.07, 0.48
M11	0.42, 0.31	0.10, 0.65
revM11	0.43, 0.39	0.23, 0.76
M11plus	0.47, 0.21	0.25, 0.37

[a]Results for the three rows above the blank row are taken from the literature; results for the four rows below the blank row are new calculations. [b]Ref 38. [c]Ref 34.

Both of the databases in Table 3 consist of excitations that were chosen to not have strong valence−Rydberg mixing or charge-transfer character. The M11plus functional does very well for the triplet excitations, although it is not quite as accurate for the singlets. The latter is probably a result of the high long-range Hartree−Fock exchange, which, however, allows it to have better performance for Rydberg excitations and charge-transfer excitations.[15]

Second-Order Response. Practical applications of the nonlocal correlation approach in M11plus will require it to be numerically robust. We next show that the new ingredients in M11plus do not make it "ill-behaved" according to the criteria emphasized by Hait et al.[39] as a measure of whether functionals predict physical spin localization in breaking bonds. We examine two response properties as functions of internuclear distance in H_2, in particular, the polarizability, which is the second derivative of the energy with respect to an applied electric field, and the local force constant, which is the second derivative of the energy with respect to internuclear distance. These properties are related because a shift in the position of a nucleus changes the nuclear Coulomb field, and the electrons respond via the same susceptibility densities that determine their response to external electric fields.[40]

Hait et al. found that some functionals show unphysical response properties when the internuclear distance R of a bond is increased past the Coulson−Fischer (CF) point, including, in some cases, secondary peaks and satellite structures in the curves of static polarizability and bond force. Figure 2 compares the isotropic static polarizability and force constant evaluated using M11 and M11plus to those evaluated for the representative "well-behaved" functional PBE and the representative "ill-behaved" functional B97-D. Arrows denote each method's CF point, that is, the first point showing non-negligible Mulliken spin density on the atoms (i.e., the first point where symmetry breaks). Section SI-8 reports all individual values.

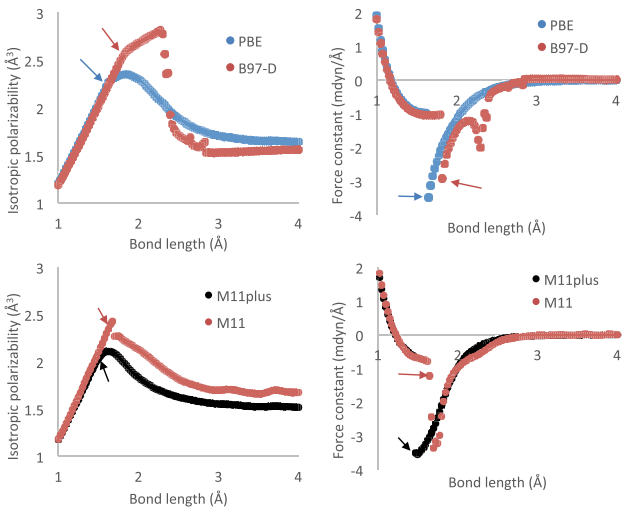

Figure 2. Isotropic static polarizability (left) and local force constant (right) for stretched H_2, plotted as functions of the H−H bond length, in spin-symmetry-broken calculations. Arrows show the first point where the symmetry breaks, that is, where the atoms have non-negligible Mulliken spin densities.

Static polarizabilities should show a kink at the CF point, heralding the start of density localization, but should otherwise be smooth. "Ill-behaved" functionals such as B97-D predict monotonically increasing static polarizability well beyond the CF point, as well as satellite peaks at long bond lengths. M11 predicts a reasonable static polarizability with only very small satellite structures at bond lengths above 3 Å. The spin-symmetry breaking occurs close to, but not always precisely at, the place where the property has an unphysical behavior. For example, for M11 at 1.675 Å, the absolute value of the Mulliken spin density on each atom is 0.0927 (unitless); however, the isotropic static polarizability is still large, being 2.43 Å^3. M11plus gives a smooth curve with a single kink at the CF point, and it is as well behaved as PBE. Furthermore, the maximum polarizability along the curve is 2.1 Å^3 at R = 1.6 Å, which is in reasonable agreement with the accurate value[41] of 1.8 Å^3 at R = 1.8 Å.

Local force constants should have a single discontinuity at the CF point and decay smoothly to zero as the bond is stretched. "Ill-behaved" functionals such as B97-D instead show additional satellite structures beyond the CF point. The M11 force constant has only a very small shoulder around 2.5 Å, and the M11plus force constant is as well behaved as PBE.

Timings. Adding nonlocal correlation to a functional typically introduces both an additional computational cost and an additional barrier toward applicability, that is, a limitation on what properties are readily computed. The nonlocal one-electron ingredients in M11plus minimize both potential drawbacks. To demonstrate this, Table 4 presents M11plus timings for computing the energies, nuclear forces, and vibrational frequencies of linear chains of 9 and 25 alanines. Elapsed times are reported relative to B3LYP, a representative and widely used global hybrid GGA, and M11, a representative long-range-corrected hybrid meta functional. Calculations use the 6-31G* basis set and a machine having 28 Intel Broadwell cores. To provide a fair "real-world" comparison, these calculations include the default integral prescreening, integration grid pruning, and SCF acceleration

https://dx.doi.org/10.1021/acs.jpclett.0c00549
J. Phys. Chem. Lett. 2020, 11, 3045−3050

Table 4. Relative Computational Timings for Alanine9 and Alanine25 Forces and Frequencies[a]

system	property	M11:B3LYP	M11plus:M11
Ala_9	energy + force	1.83	1.36
	energy + force + freq	1.60	1.24
Ala_{25}	energy + force	1.60[b]	1.28
	energy + force + freq	1.57	1.18

[a]Relative elapsed times for the convergence of the self-consistent field equations (energy), evaluation of nuclear coordinate forces (force), and evaluation of nuclear coordinate second derivatives (freq). [b]For Ala_{25}, the SCF with B3LYP takes 18 iterations, whereas M11 and M11plus require only 14. Timings have been scaled to reflect the cost per iteration.

implemented in Gaussian. Section SI-2 details specific algorithmic improvements introduced for M11plus.

M11plus incurs only a modest cost over its predecessor M11. The additional cost is smaller than that incurred on going from a hybrid GGA to a range-separated hybrid meta functional. (The M11:B3LYP cost increase arises from the separate computation of full- and short-range Coulomb and exchange integrals in M11, the less effective screening of M11 full-range exchange (coefficient 1.0) versus B3LYP full-range exchange (coefficient 0.25), and the meta (kinetic energy) terms in M11; see Section SI-2.) The M11plus scaling with system size (going from Ala_9 to Ala_{25}) is similar to that of the other functionals. The improved accuracy of M11plus does not come with some heavy burden of cost.

The results presented here indicate that M11plus is competitive with state-of-the-art modern functionals. M11plus adds nonlocal correlation to the predecessor range-separated hybrid meta functional form parametrized as M11 and revM11. The new ingredients help to give M11plus the lowest WTMAD-2 of any long-range-corrected Minnesota functional for the GMTKN55 database of thermochemistry, kinetics, and noncovalent interactions, placing it squarely in the ranks of the "best" occupied-orbital-only functionals published for this very broad state-of-the-art data set. M11plus also gives one of the lowest RMSDs reported for test sets of valence triplet excitations while maintaining reasonable accuracy for singlet excitations. Gratifyingly, these new ingredients and new parameters do not make M11plus "ill-behaved" for single bond dissociation and do not incur significant computational cost over other long-range-corrected Minnesota functionals.

Overall, these results demonstrate that rung-3.5 ingredients, which involve nonlocal one-electron operators, are useful and practical for improving the broad accuracy of even state-of-the-art range-separated hybrid meta functionals.

■ ASSOCIATED CONTENT

Supporting Information

The Supporting Information is available free of charge at https://pubs.acs.org/doi/10.1021/acs.jpclett.0c00549.

Computational methods; algorithmic issues and computational timings; Radical7 and Nonradical48 WTMAD-2 for all functionals in Figure 1; M06-2X, M11, revM11, and M11plus error statistics for all databases of GMTKN55 and MOR41; M11, revM11, and M11plus total energies and energy differences for all molecules in the GMTKN55 and MOR41 sets; state symmetries and excitation energies for all singlet and triplet excitations in the Thiel test set; energies and excitation energies for captodative chromophores; and total energies, polarizabilities, and force constants for stretched H_2 (PDF)

■ AUTHOR INFORMATION

Corresponding Author

Benjamin G. Janesko − *Department of Chemistry and Biochemistry, Texas Christian University, Fort Worth, Texas 76110, United States;* orcid.org/0000-0002-2572-5273; Email: b.janesko@tcu.edu

Authors

Pragya Verma − *Department of Chemistry, Chemical Theory Center, Nanoporous Materials Genome Center, and Minnesota Supercomputing Institute, University of Minnesota, Minneapolis, Minnesota 55455-0431, United States;* orcid.org/0000-0002-5722-0894

Giovanni Scalmani − *Gaussian, Inc., Wallingford, Connecticut 06492, United States*

Michael J. Frisch − *Gaussian, Inc., Wallingford, Connecticut 06492, United States*

Donald G. Truhlar − *Department of Chemistry, Chemical Theory Center, Nanoporous Materials Genome Center, and Minnesota Supercomputing Institute, University of Minnesota, Minneapolis, Minnesota 55455-0431, United States;* orcid.org/0000-0002-7742-7294

Complete contact information is available at: https://pubs.acs.org/10.1021/acs.jpclett.0c00549

Notes

The authors declare no competing financial interest.

■ ACKNOWLEDGMENTS

This work was supported in part by the National Science Foundation under grant no. CHE-1746186.

■ REFERENCES

(1) Kohn, W.; Sham, L. J. Self-Consistent Equations Including Exchange and Correlation Effects. *Phys. Rev.* **1965**, *140*, A1133−A1138.

(2) von Barth, U.; Hedin, L. A Local Exchange-Correlation Potential for the Spin Polarized Case: I. *J. Phys. C: Solid State Phys.* **1972**, *5*, 1629−1642.

(3) Langreth, D. C.; Mehl, M. J. Beyond the Local-Density Approximation in Calculations of Ground-State Electronic Properties. *Phys. Rev. B: Condens. Matter Mater. Phys.* **1983**, *28*, 1809−1834.

(4) Baroni, S.; Tuncel, E. Exact-Exchange Extension of the Local-Spin-Density Approximation in Atoms: Calculation of Total Energies and Electron Affinities. *J. Chem. Phys.* **1983**, *79*, 6140−6144.

(5) Becke, A. D. Density-Functional Thermochemistry. III. The Role of Exact Exchange. *J. Chem. Phys.* **1993**, *98*, 5648−5652.

(6) Proynov, E. I.; Ruiz, E.; Vela, A.; Salahub, D. R. Determining and Extending the Domain of Exchange and Correlation Functionals. *Int. J. Quantum Chem.* **1995**, *56*, 61−78.

(7) Becke, A. D. Correlation Energy of an Inhomogeneous Electron Gas: A Coordinate-Space Model. *J. Chem. Phys.* **1988**, *88*, 1053−1062.

(8) Dion, M.; Rydberg, H.; Schröder, E.; Langreth, D. C.; Lundqvist, B. I. van der Waals Density Functional for General Geometries. *Phys. Rev. Lett.* **2004**, *92*, 246401.

(9) Zhao, Y.; Lynch, B. J.; Truhlar, D. G. Doubly Hybrid Meta DFT: New Multi-Coefficient Correlation and Density Functional Methods for Thermochemistry and Thermochemical Kinetics. *J. Phys. Chem. A* **2004**, *108*, 4786−4791.

(10) Grimme, S. Semiempirical Hybrid Density Functional with Perturbative Second-Order Correlation. *J. Chem. Phys.* **2006**, *124*, 034108.
(11) Becke, A. D. Real-Space Post-Hartree−Fock Correlation Models. *J. Chem. Phys.* **2005**, *122*, 064101.
(12) Janesko, B. G. Rung 3.5 Density Functionals. *J. Chem. Phys.* **2010**, *133*, 104103.
(13) Janesko, B. G. Rung 3.5 Density Functionals: Another Step on Jacob's Ladder. *Int. J. Quantum Chem.* **2013**, *113*, 83−88.
(14) Janesko, B. G.; Proynov, E.; Scalmani, G.; Frisch, M. J. Long-Range-Corrected Rung 3.5 Density Functional Approximations. *J. Chem. Phys.* **2018**, *148*, 104112.
(15) Verma, P.; Janesko, B. G.; Wang, Y.; He, X.; Scalmani, G.; Frisch, M. J.; Truhlar, D. G. M11plus: A Range-Separated Hybrid Meta Functional with Both Local and Rung-3.5 Correlation Terms and High Across-the-Board Accuracy for Chemical Applications. *J. Chem. Theory Comput.* **2019**, *15*, 4804−4815.
(16) Janesko, B. G.; Scuseria, G. E. Local Hybrid Functionals Based on Density Matrix Products. *J. Chem. Phys.* **2007**, *127*, 164117.
(17) Becke, A. D. Real-Space Post-Hartree-Fock Correlation Models. *J. Chem. Phys.* **2005**, *122*, 064101.
(18) Zhao, Y.; Truhlar, D. G. The M06 Suite of Density Functionals for Main Group Thermochemistry, Thermochemical Kinetics, Noncovalent Interactions, Excited States, and Transition Elements: Two New Functionals and Systematic Testing of Four M06-Class Functionals and 12 Other Functionals. *Theor. Chem. Acc.* **2008**, *120*, 215−241.
(19) Peverati, R.; Truhlar, D. G. Improving the Accuracy of Hybrid Meta-GGA Density Functionals by Range Separation. *J. Phys. Chem. Lett.* **2011**, *2*, 2810−2817.
(20) Verma, P.; Wang, Y.; Ghosh, S.; He, X.; Truhlar, D. G. Revised M11 Exchange-Correlation Functional for Electronic Excitation Energies and Ground-State Properties. *J. Phys. Chem. A* **2019**, *123*, 2966−2990.
(21) Goerigk, L.; Hansen, A.; Bauer, C.; Ehrlich, S.; Najibi, A.; Grimme, S. A Look at the Density Functional Theory Zoo with the Advanced GMTKN55 Database for General Main Group Thermochemistry, Kinetics and Noncovalent Interactions. *Phys. Chem. Chem. Phys.* **2017**, *19*, 32184−32215.
(22) Dohm, S.; Hansen, A.; Steinmetz, M.; Grimme, S.; Checinski, M. P. Comprehensive Thermochemical Benchmark Set of Realistic Closed-Shell Metal Organic Reactions. *J. Chem. Theory Comput.* **2018**, *14*, 2596−2608.
(23) Iron, M. A.; Janes, T. Evaluating Transition Metal Barrier Heights with the Latest Density Functional Theory Exchange−Correlation Functionals: The MOBH35 Benchmark Database. *J. Phys. Chem. A* **2019**, *123*, 3761−3781.
(24) Zhao, Y.; Schultz, N. E.; Truhlar, D. G. Design of Density Functionals by Combining the Method of Constraint Satisfaction with Parametrization for Thermochemistry, Thermochemical Kinetics, and Noncovalent Interactions. *J. Chem. Theory Comput.* **2006**, *2*, 364−382.
(25) Grimme, S.; Antony, J.; Ehrlich, S.; Krieg, H. A Consistent and Accurate Ab Initio Parametrization of Density Functional Dispersion Correction (DFT-D) for the 94 Elements H-Pu. *J. Chem. Phys.* **2010**, *132*, 154104.
(26) Zhao, Y.; Ng, H. T.; Peverati, R.; Truhlar, D. G. Benchmark Database for Ylidic Bond Dissociation Energies and its Use for Assessments of Electronic Structure Methods. *J. Chem. Theory Comput.* **2012**, *8*, 2824−2834.
(27) Zhao, Y.; Truhlar, D. G. Exploring the Limit of Accuracy of the Global Hybrid Meta Density Functional for Main-Group Thermochemistry, Kinetics, and Noncovalent Interactions. *J. Chem. Theory Comput.* **2008**, *4*, 1849−1868.
(28) Lin, Y.-S.; Li, G.-D.; Mao, S.-P.; Chai, J.-D. Long-Range Corrected Hybrid Density Functionals with Improved Dispersion Corrections. *J. Chem. Theory Comput.* **2013**, *9*, 263−272.
(29) Mardirossian, N.; Head-Gordon, M. ωB97X-V: A10-Parameter, Range-Separated Hybrid, Generalized Gradient Approximation Density Functional with Nonlocal Correlation, Designed by a Survival-of-the-Fittest Strategy. *Phys. Chem. Chem. Phys.* **2014**, *16*, 9904−9924.
(30) Mardirossian, N.; Head-Gordon, M. ωB97M-V: A Combinatorially Optimized, Range-Separated Hybrid, Meta-GGA Density Functional with VV10 Nonlocal Correlation. *J. Chem. Phys.* **2016**, *144*, 214110.
(31) Najibi, A.; Goerigk, L. The Nonlocal Kernel in van der Waals Density Functionals as an Additive Correction: An Extensive Analysis with Special Emphasis on the B97M-V and ωB97M-V Approaches. *J. Chem. Theory Comput.* **2018**, *14*, 5725−5738.
(32) Schreiber, M.; Silva-Junior, M. R.; Sauer, S. P.; Thiel, W. Benchmarks for Electronically Excited States: CASPT2, CC2, CCSD, and CC3. *J. Chem. Phys.* **2008**, *128*, 134110.
(33) Loos, P.-F.; Scemama, A.; Blondel, A.; Garniron, Y.; Caffarel, M.; Jacquemin, D. A Mountaineering Strategy to Excited States: Highly Accurate Reference Energies and Benchmarks. *J. Chem. Theory Comput.* **2018**, *14*, 4360−4379.
(34) Grotjahn, R.; Maier, T. M.; Michl, J.; Kaupp, M. Development of a TDDFT-Based Protocol with Local Hybrid Functionals for the Screening of Potential Singlet Fission Chromophores. *J. Chem. Theory Comput.* **2017**, *13*, 4984−4996.
(35) Christiansen, O.; Koch, H.; Jørgensen, P.; Helgaker, T. Integral Direct Calculation of CC2 Excitation Energies: Singlet Excited States of Benzene. *Chem. Phys. Lett.* **1996**, *263*, 530−539.
(36) Chai, J.-D.; Head-Gordon, M. Long-Range Corrected Hybrid Density Functionals with Damped Atom−Atom Dispersion Corrections. *Phys. Chem. Chem. Phys.* **2008**, *10*, 6615−6620.
(37) Arbuznikov, A. V.; Kaupp, M. Importance of the Correlation Contribution for Local Hybrid Functionals: Range Separation and Self-Interaction Corrections. *J. Chem. Phys.* **2012**, *136*, 014111.
(38) Maier, T. M.; Bahmann, H.; Arbuznikov, A. V.; Kaupp, M. Validation of Local Hybrid Functionals for TDDFT Calculations of Electronic Excitation Energies. *J. Chem. Phys.* **2016**, *144*, 074106.
(39) Hait, D.; Rettig, A.; Head-Gordon, M. Well-Behaved Versus Ill-Behaved Density Functionals for Single Bond Dissociation: Separating Success from Disaster Functional by Functional for Stretched H_2. *J. Chem. Phys.* **2019**, *150*, 094115.
(40) Hunt, K. L. C. Vibrational Force Constants and Anharmonicities: Relation to Polarizability and Hyperpolarizability Densities. *J. Chem. Phys.* **1995**, *103*, 3552−3560.
(41) Rychlewski, J. An Accurate Calculation of the Polarizability of the Hydrogen Molecule and its Dependence on Rotation, Vibration and Isotopic Substitution. *Mol. Phys.* **1980**, *41*, 833−842.

https://dx.doi.org/10.1021/acs.jpclett.0c00549
J. Phys. Chem. Lett. 2020, 11, 3045−3050